LETTER

Evidence of ionic liquid crystal properties for a DODA$^+$ salt of the keplerate [Mo$_{132}$O$_{372}$(CH$_3$COO)$_{30}$(H$_2$O)$_{72}$]$^{42-}$†

Sébastien Floquet,*[a] Emmanuel Terazzi,*[b] Akram Hijazi,[ac] Laure Guénée,[b] Claude Piguet[b] and Emmanuel Cadot[a]

Thermal studies of a DODA$^+$ salt of the nanoscopic hollow sphere [Mo$_{132}$O$_{372}$(H$_2$O)$_{72}$(CH$_3$CO$_2$)$_{30}$]$^{42-}$ revealed ionic liquid crystalline properties, which were evidenced by Polarised Optical Microscopy, DSC and SA-XRD.

Liquid crystals constitute a fascinating example of functional self-assembled materials. Incorporation of some inorganic components into liquid crystalline phases appears particularly relevant for the elaboration of synergistic multifunctional materials according to a "bottom-up" approach.[1] To date, a large part of metallomesogens have been prepared by chemical integration of metal ions into organic ligands, which offer a large panel of materials tuned by the design of the organic part.[2] Polyoxometalates (POM), often described as polyanionic molecular oxides, exhibit a number of properties in all domains of chemistry.[3] Dietz and Wu demonstrated that the association of various POM with phosphonium or ammonium derivatives leads to ionic liquids or ionic mesomorphic self-assemblies.[4] In such a context, the "keplerate" clusters with the general formula [(Mo$_6$O$_{21}$)$_{12}$(linker)$_{30}$(Ligand)$_{30}$ (H$_2$O)$_{72}$]$^{n-}$ (Fig. 1) constitute a unique class of nanoscopic hollow spherical clusters capable of exchanging and trapping cations, especially when internal ligands are sulfates.[5] These highly charged nano-capsules can be further encapsulated by surfactants like dioctadecyl–dimethylammonium cations (DODA$^+$) to give precursors for the preparation of monolayers and Langmuir–Blodgett films,[6] useful for the functionalization of mesoporous silica[7] or for cation-trapping.[8] Taking into account the capability of
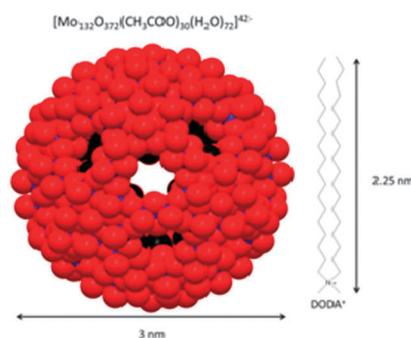
Fig. 1 Space filling representation of the spherical cluster [Mo$_{132}$O$_{372}$(H$_2$O)$_{72}$(CH$_3$CO$_2$)$_{30}$]$^{42-}$ (black: carbon, red: oxygen, blue: molybdenum) and schematic view of the DODA$^+$ cation.

changing the nature of internal ligands and the properties of the large inner cavity of the keplerate,[5,9] these spherical systems offer promising properties towards sequestration of various substrates. A result obtained with a Müller's ring-shaped compound, namely (DODA)$_{23}$ [Mo$_{154}$O$_{462}$H$_5$]·nH$_2$O, supports this expectation since adsorption of various gases and some catalytic properties of the inner open cavity are demonstrated.[10] However, to our knowledge, despite the evidence that these ionic associations easily self-assemble into organized layers or vesicles, the liquid crystal properties of keplerate-based materials were not established.

In this contribution, we present preliminary results obtained with (DODA)$_{36}$(NH$_4$)$_6$[Mo$_{132}$O$_{372}$(CH$_3$COO)$_{30}$(H$_2$O)$_{72}$]·75H$_2$O, denoted hereafter **DODA-Mo$_{132}$**, which exhibits ionic liquid crystalline properties between room temperature and temperature of decomposition, after removal of the water molecules. Syntheses of mixed DODA$^+$/NH$_4^+$ salts (DODA)$_x$(NH$_4$)$_{42-x}$[Mo$_{132}$O$_{372}$(CH$_3$COO)$_{30}$(H$_2$O)$_{72}$]·nH$_2$O were performed by extracting the anion [Mo$_{132}$O$_{372}$(CH$_3$COO)$_{30}$(H$_2$O)$_{72}$]$^{42-}$ (Mo$_{132}$) from an aqueous solution into a chloroform solution of DODACl. After extraction of keplerate into the organic phase, the final product was precipitated by addition of ethanol, isolated by filtration and washed with ethanol. Interestingly, the proportion of DODA$^+$ vs. NH$_4^+$ cations can be easily tuned as a function of the initial ratio DODACl/Mo$_{132}$ and several compounds with the DODA$^+$ content, x, ranging from 15 to 36 can be isolated when the ratio DODA$^+$/Mo$_{132}$ varies from 42 to 182. The synthesis and the

[a] *Institut Lavoisier de Versailles, UMR 8180, University of Versailles Saint-Quentin, 45 av. des Etats-Unis, 78035 Versailles, France. E-mail: sebastien.floquet@chimie.uvsq.fr; Fax: +33 139254381; Tel: +33 139254379*
[b] *Department of Inorganic, Analytical and Applied Chemistry, University of Geneva, 30 quai E. Ansermet, CH-1211 Geneva 4, Switzerland. E-mail: emmanuel.terazzi@unige.ch; Fax: +41 223796830; Tel: +41 223796035*
[c] *Lebanese University, Doctoral School of Science and Technology, Research Platform for Environmental Science (PRASE), Beirut, Lebanon*
† Electronic supplementary information (ESI) available: Experimental section; SA-XRD data in the −30 to 240 °C temperature range; FT-IR spectra; UV-Visible spectrum, TGA traces, evolution of the lattice parameter h with temperature; representation of the organization of clusters **DODA-Mo$_{132}$** in the mesophase. See DOI: 10.1039/c2nj20923c
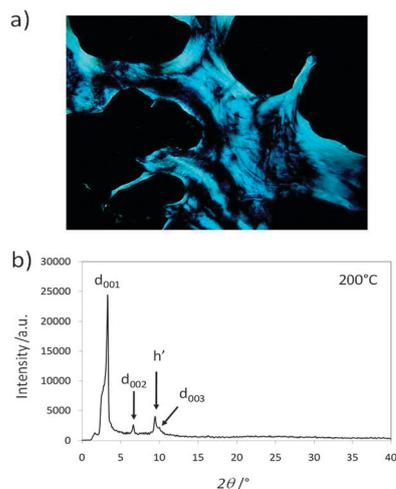
Fig. 2 (a) Fluid and birefringent optical texture (POM) of the lamellar mesophase observed for **DODA-Mo$_{132}$** at 200 °C. (b) X-Ray pattern of **DODA-Mo$_{132}$** recorded at 200 °C.
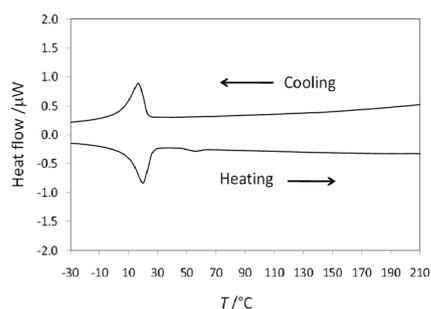
Fig. 3 DSC trace of cluster **DODA-Mo$_{132}$** (second heating and cooling at 5 °C min^{-1} under N$_2$).

Table 1 Phase-transition temperatures and enthalpy and entropy changes for DODA-Mo$_{132}$

Compound	Transition^a	T^b/°C	ΔH^b/kJ mol^{-1}	ΔS^b/J mol^{-1} K^{-1}
DODA-Mo$_{132}$	g → L	9	849	3009
	L → Dec	>260	—	—

^{a} g = glass, L = lamellar phase, Dec = decomposition. ^{b} Values are given on second heating.

usual characterizations of **DODA-Mo$_{132}$** presented in this paper are described in the ESI† (Fig. S1–S5).

Induction of mesomorphism by partially replacing ammonium with DODA$^+$ was detected for **DODA-Mo$_{132}$**. The overall structure as well as the stoichiometry of this salt is very close to that previously synthesized by Volkmer et al.[6] and by Barboiu et al.[7] Upon heating **DODA-Mo$_{132}$**, temperature dependent Polarized Optical Microscopy (POM) revealed the formation of a fluid birefringent and homogeneous texture characteristic of the liquid-crystalline nature of the sample (Fig. 2a). Combination of Thermogravimetric Analysis (TGA) and Differential Scanning Calorimetry (DSC) (Fig. S3 (ESI†) and Fig. 3, respectively) indicates that mesomorphism occurs between a first order transition at low temperature and decomposition at high temperature (above 260 °C) (Table 1). The weight loss that occurs between room temperature and 150 °C corresponds to the loss of the solvation water molecules and those located within the cavity of the cluster. Once heated above 150 °C no rehydration was found when cooling down. The lack of typical texture due to the decomposition of the cluster at high temperature before reaching the isotropic liquid precludes an unambiguous phase assignment by POM. Temperature dependent Small-angle X-ray Diffraction (SA-XRD) experiments (−30 to 260 °C) were carried out to elucidate the nature of the liquid crystalline phase. Up to three equidistant reflections indexed as the 001, 002 and 003

Miller indices (00*l*) were detected (Fig. 2b, Table 2 and Table S1, ESI†). Their sharpness indicates that they correspond to long range organizations. Such pattern is characteristic of a 1D lamellar ordering. The lamellar periodicity *h* is slightly temperature-dependent (linear dependence, 0.007 Å K^{-1}, from 60 to 260 °C, Fig. S6–S8, ESI†). At lower temperature, the decrease of the lattice parameter continues and reaches a value of 24.4(1) Å. This evolution of the lattice parameter with temperature confirms the first order transition measured by DSC. The solid state can be described as an ordered glassy state, in which the liquid crystalline phase has been frozen. According to the small change of the lattice parameter in the liquid crystalline domain, data collected at T = 200 °C were arbitrarily chosen for the discussion. A 1D lamellar ordering could appear surprising if we consider the spherical shape of the cluster. Nevertheless, as shown by a theoretical study, polyoxometalates, even in the absence of charge, prefer to form a bidimensional sheet-like structure[11] and studies of Volkmer and Barboiu clearly confirm the capability of **DODA-Mo$_{132}$** to assemble into lamellar aggregates.[6,7]

The ionic character of this material implies that the positive charges of the DODA$^+$ are necessarily located close to the negatively charged spherical surface of Mo$_{132}$. If no external constraint is applied, DODA$^+$ cations should be randomly distributed onto the surface (e.g. in solution). In the solid or liquid crystalline state, the situation could be different. If a deformation (a deviation from the spherical distribution) is required to minimize the electric multipolar interactions, the system is distorted accordingly. When the starting object is a sphere, an elongation or a compression may occur, thus leading to prolate and oblate spheroids (Fig. S9a, ESI†). These both anisometric objects have shapes compatible with a lamellar organization. As the central Mo$_{132}$ core is rigid, the

Table 2 Indexation at a given temperature for the reflections detected in the liquid-crystalline phases by SA-XRD for **DODA-Mo$_{132}$**

T/°C	$d_{hkl(\text{mes})}$/Å	I/a.u.	00l	$d_{hkl(\text{calc})}$/Å	
200	26.9	VS (sh)	001	26.9	h = 26.9 Å
	13.3	S (sh)	002	13.4	h' = 9.3 Å
	9.3	S (sh)			a_{Hex} = 54.2 Å
	9.1	S (sh)	003	9.0	
	4.5	S (br)			

$d_{hkl(\text{mes})}$ and $d_{hkl(\text{calc})}$ are the measured and calculated diffraction spacing; h is the lattice parameter of the smectic phase; I corresponds to the intensity of the reflections (VS: very strong, S: strong; br and sh stand for broad and sharp); h and $d_{hkl(\text{calc})}$ are respectively calculated according to the formula: h = 1/3 ($d_{001(\text{exp})}$ + $2d_{002(\text{exp})}$ + $3d_{003(\text{exp})}$) and $d_{hkl(\text{calc})}$ = h/l; a_{Hex} is the local hexagonal organization within the layers calculated with eqn (1). Values are given on second cooling. The additional reflection labeled h' is probably due to short contact distance between the clusters metallic cores.
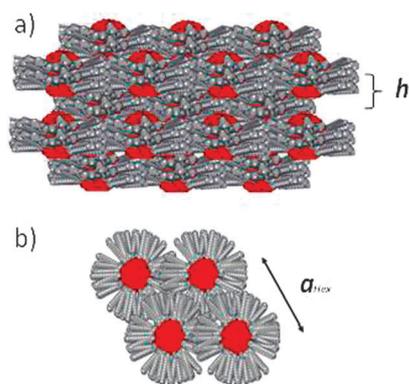
Fig. 4 Liquid crystalline organization of clusters **DODA-Mo₁₃₂**. (a) View parallel to the layers illustrating the long range layered organization. (b) View perpendicular to the layers highlighting the local hexagonal packing.

deformation can only come from the non-uniform distribution of $DODA^+$ around the keplerate (Fig. S9b, ESI†). Without being exhaustive, several examples of axial deformations of ionic liquid polyoxometallate clusters producing smectic liquid crystalline organizations can be listed.[4] However, in all cases the diameter of the anionic inorganic cores is much smaller than the lipophilic counter-cations in their unfolded conformation (about 22.5 Å). Here, the lamellar periodicity h = 26.9 Å is shorter than the central Mo_{132} core of the cluster (30 Å, estimated from the crystal structure).[9a] According to this simple consideration, a bilayer composed of prolate clusters can be excluded. We therefore conclude that the layers of the lamellar phase (L) are composed of oblate clusters (Fig. 4a). Finally, the absence of reflection corresponding to intercluster distances means that clusters are not organized within the layers. Taking into account a realistic density of d = 1.0 g cm⁻³ in the mesophase[2b] and assuming that clusters are locally ordered in a compact hexagonal lattice with one cluster per unit cell (Z = 1, Fig. 4b), we can thus calculate the hexagonal lattice parameter a_{Hex} giving an averaged inter-cluster distance of 54.2 Å, compatible with the expected dynamic diameter of the DODA-coated single nanocapsules **DODA-Mo₁₃₂** (61.8 Å)[6] and partial interdigitation of the alkyl chains of $DODA^+$ cations (eqn (1), see ESI† for the derivation of the equation; N_{AV} the Avogadro's number, MM_c the molecular weight of the cluster in g mol⁻¹, h the lamellar periodicity measured by SA-XRD, Table 1).

$$a_{Hex} = \left(\frac{2ZMM_C}{hdN_{AV}10^{-24}3^{1/2}} \right)^{1/2} \qquad (1)$$

The proposed liquid crystalline organization model is in agreement with previous studies of Volkmer,[6] who succeeded in depositing a monolayer of **DODA-Mo₁₃₂** onto a surface, and showed that clusters are organized in a 2D hexagonal lattice with a_{Hex} = 45 Å, this shorter distance being consistent with the fact that in a monolayer no constraint is applied onto the upper side of the layer.

In conclusion, we evidenced that the encapsulation of hollow keplerate Mo_{132} by $DODA^+$ cations leads to an ionic liquid crystal. These preliminary results pave the way for the encapsulation of various substrates into the cavity of this cluster, which could be tuned by the nature of their internal ligands and by the nature of the liquid crystalline phase.

Experimental

Syntheses

The synthesis of the precursor $(NH_4)_{42}[Mo_{132}O_{372}(CH_3COO)_{30}(H_2O)_{72}]\cdot300H_2O\cdot10CH_3COONH_4$ was performed as described in the literature[9a] and checked by standard methods (¹H NMR, FT-IR, UV-Visible spectroscopy). Solvents and dimethyldioctadecylammonium chloride were purchased from Acros or Aldrich Chemicals and used without further purification.

$(DODA)_{36}(NH_4)_6[Mo_{132}O_{372}(CH_3COO)_{30}(H_2O)_{72}]\cdot75H_2O$

4 g of the precursor $(NH_4)_{42}[Mo_{132}O_{372}(CH_3COO)_{30}(H_2O)_{72}]\cdot300H_2O\cdot10CH_3COONH_4$ (0.14 mmol) were solubilised in water (400 mL) to give a dark brown solution. To this solution was added a large excess of DODACl (15 g, 25.6 mmol) solubilised in chloroform (400 mL) under vigorous stirring during 3 hours at room temperature. After almost complete extraction of keplerate into the organic phase, the latter is separated by decantation and absolute ethanol (about 400 mL) is added, provoking the precipitation of the target compound as a black powder which was isolated by filtration, washed with ethanol and dried in air (m = 5.40 g, yield 90%). FT-IR/cm⁻¹ (KBr pellet, Fig. S1 and S2, ESI†): 2921(s), 2851(s), 1635(m), 1558(m), 1467(m), 981(s), 946(m), 861(s), 808(s), 732(s), 635(mw), 577(s), 471(mw). EDX: absence of Cl, which excludes the presence of an excess of DODACl in the product. Elemental analysis calcd (%) for $(DODA)_{36}(NH_4)_6[Mo_{132}O_{372}(CH_3COO)_{30}(H_2O)_{72}]\cdot75H_2O$ (M = 42 981.7 g mol⁻¹): C 39.90, H 7.71, N 1.37, Mo 29.46; found: C 39.85, H 7.51, N 1.26, Mo 29.28%. TGA under N_2 or O_2: 6.0 to 6.5% of weight loss between 20 °C and 220 °C in agreement with the loss of the 75 hydration molecules and the 72 inner aquo ligands (theoretical weight loss of 6.15%). Decomposition above 260 °C under N_2 (Fig. S3, ESI†) and above 220 °C under O_2 (Fig. S4, ESI†). UV-visible spectrum (CHCl₃, 2 × 10⁻⁵ M, Fig. S5, ESI†): λ_{max} = 469 nm, ε_{max} = 336 000 L mol⁻¹ cm⁻¹.

Notes and references

1 K. Binnemans, *Physical Properties of Metallomesogens*, in *Molecular Materials*, ed. D. W. Bruce, D. O'Hare and R. I. Walton, John Wiley & Sons, Ltd, Chichester, UK, 2010, pp. 61–141.
2 (*a*) N. Tirelli, F. Cardullo, T. Habicher, U. W. Suter and F. Diederich, *J. Chem. Soc., Perkin Trans. 2*, 2000, 193; (*b*) R. Deschenaux, B. Donnio and D. Guillon, *New J. Chem.*, 2007, **31**, 1064; (*c*) E. Terazzi, S. Suarez, S. Torelli, H. Nozary, D. Imbert, O. Mamula, J.-P. Rivera, E. Guillet, J.-M. Bénech, G. Bernardinelli, R. Scopelliti, B. Donnio, D. Guillon, J.-C. G. Bünzli and C. Piguet, *Adv. Funct. Mater.*, 2006, **16**, 157; (*d*) T. Cardinaels, K. Driesen, T. N. Parac-Vogt, B. Heinrich,

C. Bourgogne, D. Guillon, B. Donnio and K. Binnemans, *Chem. Mater.*, 2005, **17**, 6589; (*e*) R. W. Date, E. Fernandez Iglesias, K. E. Rowe, J. M. Elliott and D. W. Bruce, *Dalton Trans.*, 2003, 1914; (*f*) I. Aprahamian, T. Yasuda, T. Ikeda, S. Saha, W. R. Dichtel, K. Isoda, T. Kato and J. F. Stoddart, *Angew. Chem., Int. Ed.*, 2007, **46**, 4675; (*g*) E. D. Baranoff, J. Voignier, T. Yasuda, V. Heitz, J.-P. Sauvage and T. Kato, *Angew. Chem., Int. Ed.*, 2007, **46**, 4680; (*h*) E. Terazzi, C. Bourgogne, R. Welter, J. L. Gallani, D. Guillon, G. Rogez and B. Donnio, *Angew. Chem., Int. Ed.*, 2008, **47**(3), 490.

3 (*a*) A. Dolbecq, E. Dumas, C. R. Mayer and P. Mialane, *Chem. Rev.*, 2010, **110**(10), 6009; (*b*) A. Proust, R. Thouvenot and P. Gouzerh, *Chem. Commun.*, 2008, **16**, 1837; (*c*) D.-L. Long, R. Tsunashima and L. Cronin, *Angew. Chem., Int. Ed.*, 2010, **49**(10), 1736.

4 (*a*) P. G. Rickert, M. R. Antonio, M. A. Firestone, K.-A. Kunatko, T. Szreder, J. F. Wishart and M. L. Dietz, *J. Phys. Chem. B*, 2007, **111**, 4685; (*b*) X. Lin, W. Li, J. Zhang, H. Sun, Y. Yan and L. Wu, *Langmuir*, 2010, **26**(16), 13201; (*c*) S. Yin, H. Sun, Y. yan, W. Li and L. Wu, *J. Phys. Chem. B*, 2009, **113**, 2355; (*d*) W. Li, S. Yin, J. Wang and L. Wu, *Chem. Mater.*, 2008, **20**, 514; (*e*) S. Yin, W. Li, J. Wang and L. Wu,

J. Phys. Chem. B, 2008, **112**, 3983; (*f*) W. Li, W. Bu, H. Li, L. Wu and M. Li, *Chem. Commun.*, 2005, 3785.

5 A. Merca, E. T. K. Haupt, T. Mitra, H. Bögge, D. Rehder and A. Müller, *Chem.–Eur. J.*, 2007, **13**, 7650.

6 (*a*) D. Volkmer, A. Du Chesne, D. G. Kurth, H. Schnablegger, P. Lehmann, M. J. Koop and A. Müller, *J. Am. Chem. Soc.*, 2000, **122**, 1995; (*b*) D. G. Kurth, P. Lehmann, D. Volkmer, A. Müller and D. Schwahn, *J. Chem. Soc., Dalton Trans.*, 2000, 3989.

7 A. Cazacu, S. Mihai, G. Nasr, E. Mahon, A. van der Lee, A. Meffre and M. Barboiu, *Inorg. Chim. Acta*, 2010, **363**, 4214.

8 H. Li, Y. Yang, Y. Wang, C. Wang, W. Li and L. Wu, *Soft Matter*, 2011, **7**, 2668.

9 (*a*) A. Müller, E. Krickemeyer, H. Bögge, M. Schmidtmann and F. Peters, *Angew. Chem., Int. Ed.*, 1998, **37**(24), 3359; (*b*) A. Ziv, A. Grego, S. Kopilevitch, L. Zeiri, P. Miro, C. Bo, A. Müller and I. A. Weinstock, *J. Am. Chem. Soc.*, 2009, **131**, 6380.

10 S. I. Noro, R. Tsunashima, Y. Kamiya, K. Uemura, H. Kita, L. Cronin, T. Akutegawa and T. Nakamura, *Angew. Chem., Int. Ed.*, 2009, **48**, 8703.

11 E. Mani, J. Groenewold and W. K. Kegel, *Inorg. Chim. Acta*, 2010, **363**, 4295.